ELSEVIER

Chemical Geology 230 (2006) 220–231

CHEMICAL GEOLOGY
INCLUDING
ISOTOPE GEOSCIENCE

www.elsevier.com/locate/chemgeo

Confined fluids and their role in pressure solution

Alessandro Anzalone [a], James Boles [c], George Greene [b], Kevin Young [a], Jacob Israelachvili [b], Norma Alcantar [a,*]

[a] *Department of Chemical Engineering, University of South Florida, Tampa, FL 33620, USA*
[b] *Department of Chemical Engineering and Materials Science Department, University of California, Santa Barbara, CA 93105, USA*
[c] *Department of Geology, University of California, Santa Barbara, CA 93105, USA*

Accepted 2 February 2006

Abstract

The process of pressure solution is defined as the dissolution of materials under high stress at grain-to-grain contacts and precipitation at interfaces under low stress. The kinetics of this process are still poorly understood mainly because of the large timescales involved. In this research, the Surface Forces Apparatus (SFA) technique was coupled with an optical interference technique for in situ visualization of the nanoscale deformations and thickness changes. The SFA was used to measure the forces (or pressures) and distances between two solid surfaces pressed together with a thin film between them. Using the SFA, combined with geological observations, we are studying the short-range colloidal forces between surfaces of mica and silica at the nanoscale such as van der Waals, electrostatic, and hydration forces.

This study involves two cases, the symmetric case of mica in contact with mica and the asymmetric case of a quartz surface in contact with mica. Our results reveal highly subtle effects depending on the nature and concentration of the counterions present in the solution either of Na^+, Ca^{2+}, or mixtures of these ions, as well as on the pH. For the symmetric case, the equilibrium interactions of force F or pressure P versus fluid film thickness T have been measured between the mica surfaces across aqueous films in the thickness range from $T=25$ Å down to contact separations around $T=0$ Å, and depend on the solution conditions and applied lithostatic pressure. Measurements have also been made of the rates of diffusion of ions through such ultra-thin films and on the precipitation and growth of ionic crystallite layers on the surfaces. Our results show that the diffusion coefficient of hydrated sodium is two orders of magnitude lower than the diffusion of water into mica–mica cleavage and a factor of 40 lower than the coefficient of sodium ions in bulk water.

For the asymmetric case, the dissolution of the quartz surface was observed to be dependent on the interfacial fluid composition and pH, the externally applied 'lithostatic' pressure, and the type of crystalline structure exposed to the mica surface. Our experiments also show that there is an initial stage after fresh solution is added in which the spacing between the surfaces increases, however, the thickness started decreasing steadily after approximately 4 h of exposure independently of the crystallinity of the quartz surface. For a particular set of conditions, the process eventually slows down and reaches equilibrium after some time, but a further increase in pressure restarts the dissolution process. This is also true for the addition of fresh interfacial solution during the experiment after a period of thickness fluctuation. These results are consistent with the observation that pressure solution of quartz is greatly enhanced with the presence of mica.

* Corresponding author. Tel.: +1 813 974 8009; fax: +1 813 974 3651.
E-mail address: alcantar@eng.usf.edu (N. Alcantar).

0009-2541/$ - see front matter © 2006 Elsevier B.V. All rights reserved.
doi:10.1016/j.chemgeo.2006.02.027

1. Introduction

1.1. Pressure solution

Fluids confined between mineral interfaces are ubiquitous in the natural world and are of great interest for their geological influence and fundamental physico-chemical properties at the submicroscopic and molecular levels. Those events are not well understood even though there is a considerable amount of data on interfacial phenomena at mineral surfaces in free solution (Pashley, 1982; Kekicheff et al., 1993; Hochella, 1995). Fluids under confinement play a very important role in pressure solution where processes such as the dissolution at stressed surfaces, diffusive transport of dissolved matter, and precipitation at less stressed surfaces are the result of pressure solution interfacial mechanisms. Also, the interpenetration of rocks, the dissolution of quartz in contact with mica, and on a larger scale, the development of stylolites results from the preferential dissolution of minerals along stressed grain boundaries (Heald, 1955; Tada et al., 1987; Bjørkum, 1996).

The broad explanation is that a thin film of water confined between clay and crystal surfaces triggers what is recognized as pressure solution phenomena. Three accepted models have been developed to explain their mechanisms (den Brok, 1998; Renard et al., 1999) (Fig. 1). Briefly, the Water Film Diffusion (WFD) model describes an absorbed water film layer where mineral dissolution at the grain–grain contact area results in the precipitation of minerals on the adjacent free grain surface (pore). Dissolution at the contact is stress enhanced owing to a difference of normal stress between the grain intersection and the pore. The second model relates to the Free Face Pressure Solution (FFPS) where dissolution starts at the edge of the contacts and creeps to the core by developing an attenuated brittle or plastic deformation within the mineral contacts. Thus, dissolution at the contact is strain enhanced. The third model assumes that the mineral contact contains channel and island structures ranging from the nanometer to the micron-scale that induce plastic or brittle deformations. All of these models assume that if the water film becomes very thin its structuring will limit diffusion rates.

One important characteristic in the models of pressure solution is the nature of the thin water film that is assumed to facilitate chemical reactions, be a transport medium, and have a stress dependent thickness. Additionally, the water film must be present so that large gradients can exist between the grain-contact stresses and the fluid pressure in the pore. Thus, the diffusion coefficient of solutes along this film is expected to be higher than the coefficient of diffusion in solids (Renard and Ortoleva, 1997).

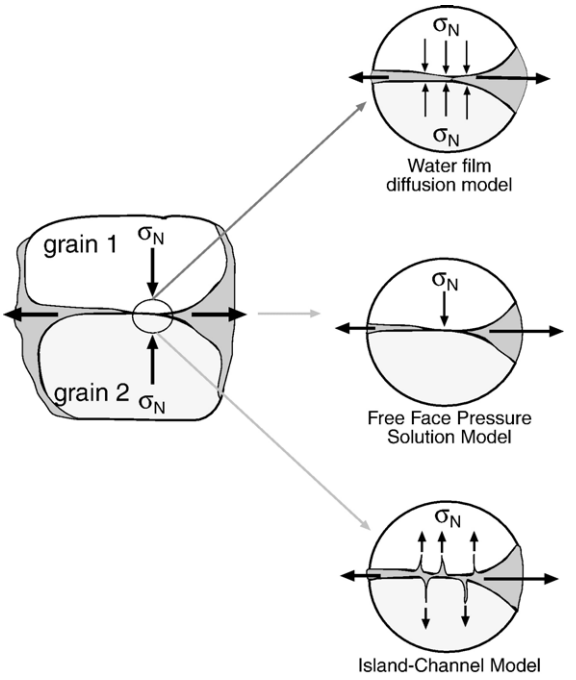

Fig. 1. Proposed models of pressure solution after (den Brok, 1998; Renard et al., 1999). Vertical arrows refer to normal pressures or crack propagation directions. Horizontal arrows refer to material transport.

The objective of this paper is to elucidate the role of clays like mica in the pressure solution of quartz. Some authors attribute the effect of quartz dissolution to thicker water films associated with mica–quartz contacts (Weyl, 1959; Rutter, 1983; Kruzhanov and Stöckhert, 1998). However, clays such as kaolinite and chlorite do not seem to promote quartz dissolution, which appears inconsistent with the idea of the importance of an enhanced water film. We have initially characterized the mica–fluid–mica interface in close contact (Alcantar et al., 2003). A summary of this work will be presented later in the paper and used to explain how fluid composition plays an important role in the behavior of dissimilar minerals. In addition, the effect of confined fluids and their composition in the mica–quartz system will be used to describe the effects of lithostatic pressure and surface structuring on the crystal dissolution rates.

1.2. The Surface Forces Apparatus technique

We have used the Surface Forces Apparatus (SFA) to determine the range of hydration (water structure-

dependent) forces, the thickness of thin aqueous films, surface strain, and the diffusion and dissolution rates between surfaces of mica and quartz while mimicking geological conditions. The SFA can measure intermolecular forces including van der Waals, electrostatic, hydration (water structure-dependent), and steric (finite ion size-dependent) interactions, which depend both on the nature of the surfaces (e.g., their chemistry, ion-exchange capacity and whether amorphous or crystalline) and the type of solution (e.g., concentration of salt present and pH).

The Surface Forces Apparatus technique (Israelachvili and Adams, 1978) is conceptually similar to atomic force microscopy (AFM) or any other mechanical force-measuring technique that employs a cantilever spring to measure forces and a series of springs and piezoelectric crystals to control surface separations. What separates the SFA from AFM and similar techniques is that the distance between surfaces is determined by an optical technique independent of the force measuring mechanisms. This optical technique, Multiple Beam Interferometry (MBI) is based upon the interferometer formed by two opposite silver mirrors in the backside of the surfaces in study (Israelachvili, 1973). MBI fringes, known as Fringes of Equal Chromatic Order (FECO), are used to accurately and unambiguously measure the absolute surface separation D to 1 Å resolution as well as the mean refractive index n of the liquid or solid film (of thickness D) between the surfaces (Israelachvili, 1973). These interference fringes are the same as observed in a quartz wedge in a petrographic microscope (Alcantar et al., 2003). By recording the changing FECO fringe pattern with time using a video camera recording system any changes in these parameters can be visualized and monitored at the angstrom-level (10^{-10} m), thus providing direct information of the force F or pressure P between two curved or flat surfaces, film thicknesses, optical activity, and surface morphology (Heuberger et al., 1997). As a consequence, ionic diffusion rates and changes in local stresses over finite periods of time can also be determined. For instance, if we record with the SFA a decrease in the thickness of 15 nm in one of the surfaces studied over a period of 4 h this translates to measure a rate of diffusion of products from the surface dissolution process of the order of 10^{-12} m/s. This is very interesting because it means that geological phenomena that vary in ranges of 25 mm in 800 years (25 mm/800 years = 10^{-12} m/s) can be monitored in the laboratory with the SFA technique during the course of an experiment. Consequently, the role of thin confined films in the deformation of rocks in the earth's crust by pressure solution can be accurately reproduced in the laboratory with the expectation of understanding how the mineral crystals, and their interactions, are responsible for the visible viscous creep of the rocks (Fig. 2).

1.3. The role of molecular diffusion

The development and understanding of molecular diffusion in confined fluids between mineral surfaces can be described by the thin water film and its effects as a semi permeable membrane, as a charge carrier, or as a corrosion vehicle at the interface. The properties of this film include the fact that the ionic concentration under confinement may be higher than the fluid concentration in the bulk and charged species (such as Na^+, Ca^{2+}, or Cl^-) create an osmotic pressure effect in the film that counteracts the contact stress. Therefore, molecular diffusion depends on the electric surface charge and the stability of the film structure that is caused by an osmotic force (Renard and Ortoleva, 1997).

The two forces that depend on the surface charge density or electric potential of the surfaces and on the bulk dielectric properties of the media are the repulsive electrostatic "double-layer" force (based on the Poisson-Boltzmann equation) and the attractive van der Waals force (based on the Lifshitz theory). The so-called Derjaguin-Landau-Verwey-Overbeek (DLVO) theory of colloidal stability (Verwey and Overbeek, 1948) describes long-ranged colloidal forces and is a non-specific, 'continuum' theory that overlooks the discrete molecular nature of the surfaces or solvent at separations greater than 20–50 Å and/or in dilute electrolyte solutions (Israelachvili, 1991). Conversely, at smaller surface separations, the DLVO theory breaks down. Non-DLVO forces appear to depend on the specific nature of the surfaces (chemically and physically) and the solution conditions (type and concentration of electrolyte, pH, and temperature). These forces have been extensively reviewed for clay and mineral systems in Pashley (1981), Pashley and Israelachvili (1984) and Israelachvili (1991).

A deeper understanding of pressure solution mechanisms and mineral surface interactions requires knowledge of "steric-hydration" from previous experiments (Alcantar et al., 2003). That is the confinement of water molecules to surfaces produces an additional repulsion in both monovalent and divalent electrolyte solutions and increases the apparent strength of the repulsive electrostatic force from the protruding charged groups that occur on amorphous silica surfaces (van Olphen, 1977; Pashley, 1981; Christenson et al., 1982; Viani et al., 1983; Pashley and Israelachvili, 1984; Kjellander et al., 1988). Other non-DLVO forces that produce additional short-range attractive interactions (Frens

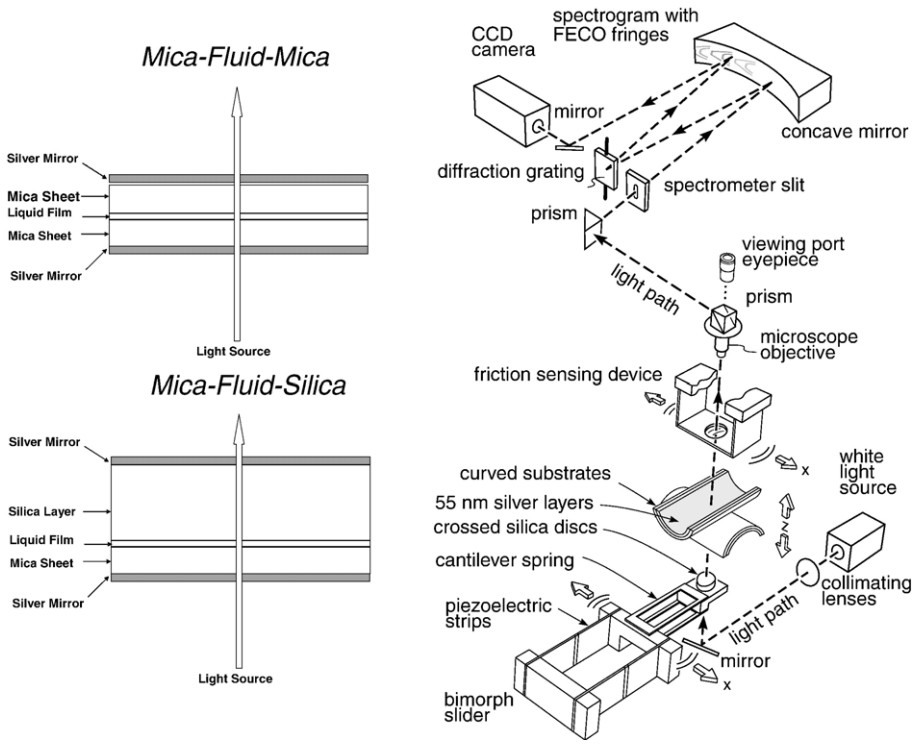

Fig. 2. Schematic representation of Surface Forces Apparatus (SFA) showing the diagrams of the interferometers produced for these experiments. The SFA technique is used to measure the force F as a function of the surface separation D (the distance of closest approach in the case of two curved surfaces). In the present study, more highly curved surfaces (lower R values) were often used to obtain lower flattened areas A and, therefore, higher pressures $P=F/A$ under a given force or load, F.

and Overbeck, 1972; Pashley, 1982; Vigil, Xu et al., 1994) are known as ion-bridging effects and result from polarizable *counterions* but are not included in the Lifshitz theory of van der Waals forces (van Olphen, 1977; Viani et al., 1983; Guldbrand et al., 1984; Pashley and Israelachvili, 1984; Kjellander et al., 1988; Kjellander et al., 1990; Kekicheff et al., 1993; Leckband and Israelachvili, 2001).

Very little systematic or detailed work has been done to measure diffusion mechanisms between dissimilar surfaces, either experimentally or theoretically, because it is necessary to determine and monitor the characteristics of the interacting surfaces such as their roughness, local geometry, and force–distance profiles with an accuracy of about 1 Å. This is precisely the sort of information that can be obtained with the SFA technique.

2. Experiments

2.1. Surfaces and solutions

Since the scope of this paper is to describe the effects of confined fluids in pressure solution special care has been taken to mimic geological studies at the molecular contact between mica–fluid–mica and mica–fluid–quartz systems. We will present the force vs. distance (or pressure–distance) profiles at several pressures showing short-distance regimes under geological pore water conditions. In the case of the mica–fluid–mica system, solutions of NaCl and $CaCl_2$ in the range 6–600 mM NaCl and 6–30 mM $CaCl_2$ were used as both pure and mixed electrolyte solutions. The pH was typically between 6 and 7 but a few measurements were also done at much lower and much higher pH. The water was sometimes purged with nitrogen gas to remove dissolved CO_2 (Alcantar et al., 2003). With the mica–fluid–quartz system, 30 mM solutions of $CaCl_2$ were used at neutral pH or acidulated with nitric acid to pH 3.8. Control solutions of HNO_3 alone at pH 3.8 were used as a comparison. Applied pressures P ranged from 2 to 50 MPa (20–500 atm). These solution conditions were chosen because they showed the most pronounced adhesion and fastest ion diffusion rate between mica–mica surfaces compared with previous observations. Measurements for both systems were conducted at 21 °C.

Freshly cleaved muscovite mica sheets of thickness 2–3 μm (ideal formula: $KAl_2[Al,SiO_3]–O_{10}[OH]_2$) were used as previously described (Israelachvili and Adams, 1978). One of these mica sheets was placed in contact with thin quartz in the SFA. Quartz sheets (MTI Corp.) were obtained by polishing one side of a thicker piece of quartz to a certain thickness as described later in the procedure section. The sheets were glued to cylindrically curved silica disks, each of radius R, and mounted in the SFA in a "crossed cylinder" configuration which is equivalent to a sphere of radius R approaching a flat, planar surface.

2.2. Experimental procedure

Sets of experiments were performed, each of them using mica against mica or mica against quartz surfaces depending on the experiment, in an SFA model Mark III and monitored using a Silicon Intensified Target (SIT) camera. The video images were recorded on Super VHS and digitized in order to perform the measurements required for the calculations. Once a digital image was available the surface position was determined from the FECO fringes by measuring the pixel position and calculating the wavelength of each fringe of interest using as reference the green and yellow lines of a mercury lamp. Usually the lower disk held the mica surface and the upper disk held either mica or thin centered-glued flat sheets of quartz.

The quartz surface was prepared by reducing one of the optically polished sides of a thicker piece of silica (originally 100 μm thick) with a Hyprez flat lapping machine starting with polishing pads (used in decreasing order from 15 μm to 1 μm grain size) and finishing with a soft-cloth surface and diamond slurries (0.2 μm Ra and 0.5 μm Ra surface finishing). Special care was taken in controlling the horizontal orientation of the quartz crystal normal to the polishing surface. However, some samples showed a slight variation in the thickness that was corroborated by environmental SEM. Nonetheless, the SFA technique allows one to measure such variation in the contact position and to account for it in the determination of the separation distance.

The surfaces were glued on transparent mounting disks with cylindrical curvature of ca. 1.5 cm radii. The initial contact position was obtained under dry conditions and verified by Newton rings on the contact area between mica–mica sheets and between mica and the center of the quartz sheet. The mica surfaces were freshly cleaved, wire cut, and back silvered. They showed a smooth adhesive contact. The quartz side in contact with the mica surface was the side optically polished from the manufacturing company. The other side was coated with the reflecting silver layer to form the interferometer. The mica thickness for our experiments varied from 3 to 4 μm. We used two sources for the silica surfaces; pieces of quartz from a Z-cut[1] crystal and fused silica sheets polished down from 100 to 8 and 17 μm, respectively.

After mounting the surfaces into the SFA chamber, it was purged with clean, dry nitrogen gas and then filled with distilled water. The surfaces were then brought into contact with one another. After establishing that the contact was adhesive and perfectly flat across the whole contact circle (no particles in the contact zone), the zero of distance, $D=0$ for the system, was recorded from the positions (wavelengths) of the straight FECO fringes (Israelachvili, 1973). The surfaces were then separated and the electrolyte and pH were then changed in succession, each time measuring the colloidal forces between the surfaces on approach and separation, their adhesion, and accompanying surface deformations. In some cases, the solution in the chamber was changed while the surfaces were kept pressed together under a large force. By monitoring the way the film thickness and contact area changed with time, it was possible to follow the rate of ion diffusion into or out of the gap as well as establish the changing stresses around the contact junction from the changing shapes of the surfaces. In other measurements, two surfaces were allowed to remain close together for a long time (hours) to see whether surface dissolution or crystal growth occurred around the contact region.

The contact areas were usually large in the quartz experiments and had an elliptical shape (contact diameter 250–350 μm) due to the flat nature of the quartz layer. No other contact position or adhesion between the two layers was observed.

2.3. Calculation of force, diffusion measurements, and thickness

In a typical "force-run," the force F is measured as a function of surface separation D between two cylindrically curved surfaces of radius R. When the forces are weak (usually colloidal DLVO-type forces at long-range), one generally plots the results as F/R versus D. This enables comparison with other measurements using surfaces of different radii since all colloidal forces are theoretically expected to scale linearly with their radius R (Israelachvili, 1991). In addition, one may plot

[1] Z cut refers to a quartz sheet with the major surface of the sheet perpendicular to the Z crystallographic axis.

pressure versus separation distance by using the well-established 'Derjaguin Approximation' (Israelachvili, 1991), which relates the forces between curved and flat surfaces according to

$$F(D)/R = 2\pi E(D) \quad \text{for } D \ll R \tag{1}$$

where $F(D)$ is the force–distance function between the two curved surfaces of radius R and where $E(D)$ is the corresponding energy–distance function between two flat (plane parallel) surfaces per unit area. The pressure at D is then obtained by differentiating $E(D)$ with respect to D:

$$P(D) = \mathrm{d}E(D)/\mathrm{d}D = \mathrm{d}(F/2\pi R)/\mathrm{d}D. \tag{2}$$

Significant flattening of the surfaces occurs at pressures above 10 atm over an (directly measurable) area A or separations below ~20 Å. In this case, one can plot $P=F(D)/A$ versus D, which gives the pressure as a function of water film thickness D.

Eq. (1) was also used to determine the adhesion energy E_0 per unit area from the measured adhesion or "pull-off" force F_{ad} needed to detach the surfaces from adhesive contact (from or close to $D=0$):

$$E_0 = F_{ad}/2\pi R. \tag{3}$$

The diffusion equation

$$\langle x \rangle^2 = Dt \tag{4}$$

was used to estimate the diffusion coefficient D of ions diffusing a distance x through the thin water films over a time t. These parameters were measured by recording the change in the FECO fringe patterns position with time.

Finally, the thickness of the quartz layer was calculated using contact information, the thickness of the mica layer, and the following equation (Israelachvili, 1973).

$$4(\mu_1 Y + \mu_3 T) = n\lambda. \tag{5}$$

2.4. Surface morphology and chemical characterization techniques

Environmental Scanning Electron Microscopy (E-SEM) was used to characterize the quartz and mica surfaces before and after the experiments. An FEI Co. XL30 ESEM with a field emission gun (FEG) was used. The E-SEM was used because it prevents charging problems common in mica and quartz samples when using a normal SEM due to their low electrical conductivity. It was used in the wet mode, i.e. moderate vacuum, where the sample chamber was flooded with water vapor, and the condensation on the specimen surface was managed via a temperature-controlled Peltier stage. The water vapor neutralizes any charge that builds up on the sample surfaces and as a result, it was not necessary to coat the surfaces with a conducting material. Thus, samples were imaged in their native state.

A Philips X'PERT X-ray Diffractometer (XRD) was used primarily for determining crystal diffraction of the quartz surfaces. The X-ray beam is at 1.5405 Å wavelength with two incident beam optics. The instrument has a panalytical X'celerator detector for high-speed XRD measurements.

Both X-ray Photoelectron Spectroscopy (XPS) and Secondary Ion Mass Spectroscopy (SIMS) (Gardella, 1995; Sherwood, 1995) were used to identify the composition of species present on the mica and quartz surfaces. For instance, in our previous work we primarily identified the formation of crystals in mica–mica contacts. SIMS was used to corroborate the findings obtained with XPS and confirmed the existence of Ca on the surfaces and in the nucleated crystals (Alcantar et al., 2003).

3. Results and analysis

We describe the results of experiments on mica and quartz aimed at identifying and quantifying some of the outstanding issues that relate dissimilar mineral surface interactions at the molecular level to pressure solution. Earlier studies focused mainly on the long-range DLVO interactions between symmetric mica surfaces in pure (single-component) electrolyte solutions (Israelachvili and Adams, 1978; Pashley, 1981; Pashley and Israelachvili, 1984; Christenson et al., 1987; Kjellander et al., 1988). Here, we will show the effects of the repulsive and attractive forces on the stresses and deformations they induce on the mineral surfaces, the diffusion and binding/exchange rates of (hydrated) ions into and out of ultra-thin water films, the precipitation and rate of growth of calcium carbonate crystals on or between two mica surfaces, and the direct observation of quartz dissolution when in contact with mica.

3.1. Mica–fluid–mica system

This brief section refers to our previous work. We have analyzed short-distance pressure–distance profiles between various mica surfaces in different solutions of pure NaCl between 6 and 600 mM and have observed that when the ionic strength of the electrolyte solutions

increases above 1 mM, the hydration repulsion steadily increases until it reaches saturation (~60 mM). Calcium and other divalent cation solutions were observed to behave quite differently from sodium and other monovalent cation solutions since pure calcium solutions enhance attractive and adhesive forces above what is expected from the Lifshitz theory of van der Waals forces by short and medium range "ion correlation forces"(Kekicheff et al., 1993; Kruzhanov and Stöckhert, 1998; Leckband and Israelachvili, 2001).

In the case of mixed NaCl–$CaCl_2$ systems the mixed solutions behave qualitatively between the two pure solutions but there are quantitative subtleties that arise from the competitive nature of the binding of Na and Ca ions to mica and antagonistic effects of these ions that greatly affect the contact adhesion and short-range hydration forces. That is, calcium ions (Fig. 3) at 6 mM exhibit a saturated hydration at much lower concentrations than sodium cations due to its thick hydration shell. From these results, we deduce that the hydration force appears to be due to the binding of hydrated cations to negatively charged clay surfaces above some "critical hydration concentration" and depends on the type of ion, the nature of the surface, and the pH (Pashley, 1981; Pashley and Israelachvili, 1984).

Fig. 4 shows the effects of ion diffusion (Na^+) and ion correlation forces (Ca^{2+}) into and out of thin water films by in situ monitoring of the change of film thicknesses, contact areas, and forces with time after a change in the solution conditions. We were able to distinguish the diffusion from the rates of ion binding, unbinding, or exchange with the surfaces. These phenomena happened in both pure and mixed NaCl and $CaCl_2$ solutions. Since the externally applied force remained constant during this swelling process, the reduction in the contact area resulted in an effective increase in the *mean* pressure at the junction, rising from 3.2 MPa at $t=0$ to 14.0 MPa at $t=14$ sec for pure 6 mM NaCl solutions when the swelling was more or less complete. Also, the penetration of hydrated sodium ions into a mica–mica contact junction occurs rapidly at the beginning when the separation distance is initially thinner than the diameter of a hydrated sodium ion (~4–7 Å).

Applying Eq. (5) to the results of Fig. 4 gives us an estimate for the diffusion coefficient of hydrated sodium ion penetration of $D \approx (20\times10^{-6})^2/14 \approx 3\times10^{-11}\,m^2/s$, which is two orders of magnitude lower than the diffusion of water into mica–mica cleavage (cracks), $D \approx 3\times10^{-9}\,m^2/s$ (Wan et al., 1992).

On the other hand, when 30 mM $CaCl_2$ is added to the 6 mM NaCl solution, the short-range repulsive hydration force grows in magnitude and range instantly increasing the steady state film thickness for NaCl from $D=8$ Å to $D=23$ Å (at $t\approx0$ s). However, this interaction is then counteracted by the attractive ion-correlation force making the film thickness decrease and the contact area increase. In further contrast to the situation with pure NaCl solutions, the contact area remained flat throughout the "collapse" rather than having different

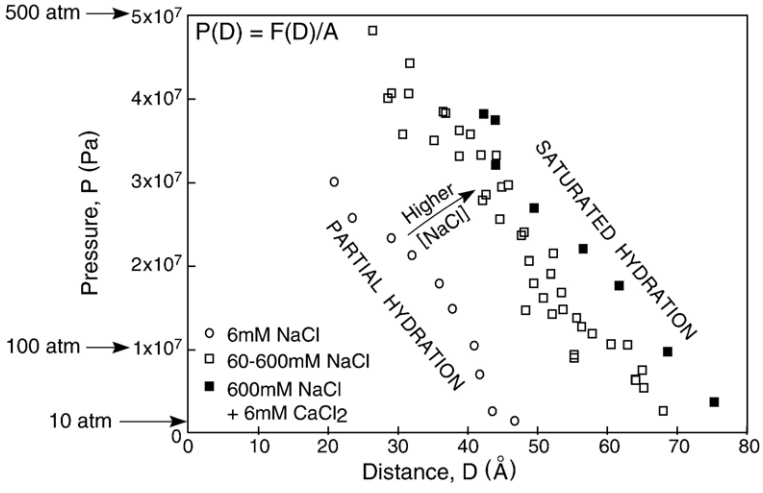

Fig. 3. Measured compressive pressures P as a function of water film thickness D under different solution conditions in pure NaCl solutions. If we were to compare our findings with the theoretically expected DLVO forces we would have seen them close to the 10 atm line (Alcantar et al., 2003). These results show that due to the binding of hydrated Na^+ ions the hydration force saturates between 6 and 60 mM NaCl (points ○ and □, respectively) and it does not increase between 130 and 600 mM NaCl (also shown as □). If 6 mM $CaCl_2$ is added to the 600 mM NaCl solution (shown as ■), the saturation line slightly increases due to the thick hydration shell of Ca^{2+}.

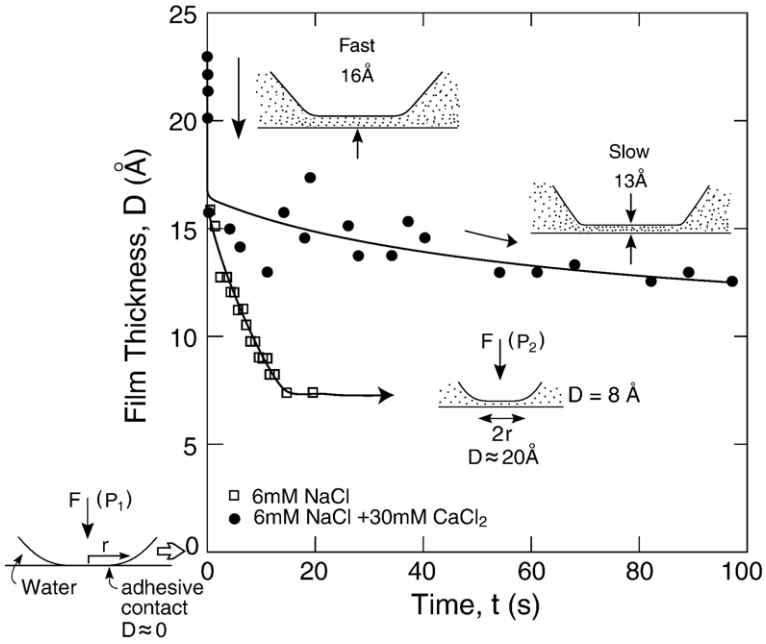

Fig. 4. The swelling of a water film from $D=0$–2 Å to $D=20$ Å is caused by raising the solution ionic strength from 0 to 6 mM NaCl while the surfaces were kept under a high pressure, 32 atm (shown as □). The reduction of the "contact" radius r with time arises from the penetration of sodium ions into the gap and produces the growth of a hydration layer and force, the separation of the surfaces to 20 Å, and the elimination of the adhesion force. The resulting effects of increasing the double-layer and ion-correlation forces are determined when 30 mM $CaCl_2$ solution are introduced in the solution (shown as ●). In contrast to the case shown in the pure system, the film thickness (which had a finite value of 23 Å at $t=0$) *decreased* and the contact radius *increased* (slightly) with time.

regions change their local thickness at different times (Alcantar et al., 2003). This transition appears to happen in two stages, a fast and a slow rate, attributed to the fast rate of diffusion of calcium ions into the gap and the calcium ions binding/exchanging with the previously bound sodium ions, respectively. We obtain two diffusion coefficients for Ca^{2+}, a fast one of $D\approx 4\times 10^{-10}\,m^2/s$ and a slow one of $D\approx 6\times 10^{-12}\,m^2/s$. The fast event is a factor of two slower than its diffusion in bulk water measured to be $D=8\times 10^{-10}\,m^2/s$ at 25 °C (Li and Gregory, 1974), however, the rate of ion binding or exchange is much slower.

This agrees with our observations of crystal growth between clays in real time. That is, small crystallites could be seen to grow either at the edges or within a contact junction in the presence of calcium. These would nucleate or precipitate quickly (seconds to minutes) from an initially totally flat contact junction in adhesive contact in dilute monovalent salt solution to a 24 Å-high crystallite inside the junction within 2 h, then grow much more slowly (days). From the FECO measurements, such crystals have a refractive index of 1.5 ± 0.1, which is comparable to calcite or aragonite since their refractive index is 1.49–1.68. We also mentioned in our previous work the physical and chemical characteristics of these crystals with XPS and SIMS (not shown). These results clearly show the presence of calcium and carbonate ions inside the contact junctions in which crystallites had grown (Alcantar et al., 2003).

3.2. Mica–fluid–quartz

The results of dissimilar surfaces are different from that of similar surfaces. The analysis of the FECO fringes for the mica–quartz case was performed by approximating the system to an asymmetrical two-layer interferometer. Some of the parameters that were determined for the symmetric mica–mica system were not determined for the mica–quartz system such as refractive index of the interfacial media between the surfaces, owing to the fact that the quartz layers were much thicker than mica sheets, lowering considerably the resolution of the MBI technique. However, we were able to calculate the thickness of the quartz layers by using Eq. (5). These values were confirmed with E-SEM images of the edge of the polished quartz and fused silica pieces before placing them in contact with any electrolyte solutions (i.e. thickness of quartz from a Z-cut crystal = 8 μm and thickness of fused

silica sheet = 17 μm). Crystallographic orientation and crystallinity of the quartz and fused silica sheets were analyzed by X-ray diffraction–XRD patterns. It was confirmed that the Z cut presented hexagonal habit with $a = 4.914$ Å and $c = 5.405$ Å. The fused silica sheet was verified to be amorphous. The equation used to calculate the change in thickness of the quartz and fused silica layers is the following (Israelachvili, 1973):

$$\Delta T = \frac{\lambda_0 \Delta\lambda}{2\mu_3 \Delta\lambda_0}. \quad (6)$$

To analyze and compare the effects of electrolyte type, lithostatic pressure, and pH in these systems to the mica–fluid–mica system, the surfaces were first exposed to pure $CaCl_2$ (30 mM) solutions at neutral and acidic pH at low (2 MPa), intermediate (32 MPa) and high (50 MPa) pressures (Fig. 5).

First, the mica against quartz and mica against fused silica surfaces were placed in the SFA, the contact position was determined in air, and 150 ml of 30 mM $CaCl_2$ were injected into the SFA. The pressure used was just above contact (2 MPa). The contact area had an elliptical shape (average diameter ≈ 250–300 μm). After the solution was injected, the FECO fringes moved towards higher wavelengths indicating separation of the surfaces. That is, the surfaces were pushed out during the injection of the electrolyte solution because it rushes into the contact area since the pressure was not high enough to maintain the surfaces in close contact. This movement corresponds to about half a fringe (1000 Å) in both cases until no noticeable movement of the fringes was detected (ca. 5 h and 22 h for fused silica and quartz, respectively).

Since no change in the separation of the surfaces was observed over the next 30 min for mica–fused silica system and 2 h for the mica–quartz system, the pressure was increased to 32 MPa. The position of the fringes started moving towards lower wavelengths immediately, indicating a decrease in thickness. In the case of fused silica, a rapid decay in the thickness was recorded until it reached a constant value after 14 h of contact. This time period includes the removal of hydrated ions in between the surfaces and indicates a significant dissolution of the fused silica surface when in contact with mica (ca. 5500 Å). For the quartz surface, we observe approximately a 400 Å net decrease in thickness at this pressure when the surfaces approached to a plateau region near the 45 h mark. The pressure was again raised to the maximum pressure allowed of 50 MPa. Previous experiments have not only indicated that higher pressures might result in quartz cracking at the contact position but also that the large area of contact between the dissimilar surfaces influences the surface pressure even though a stiff spring is used. The dissolution rate increased again after raising the pressure. The surfaces

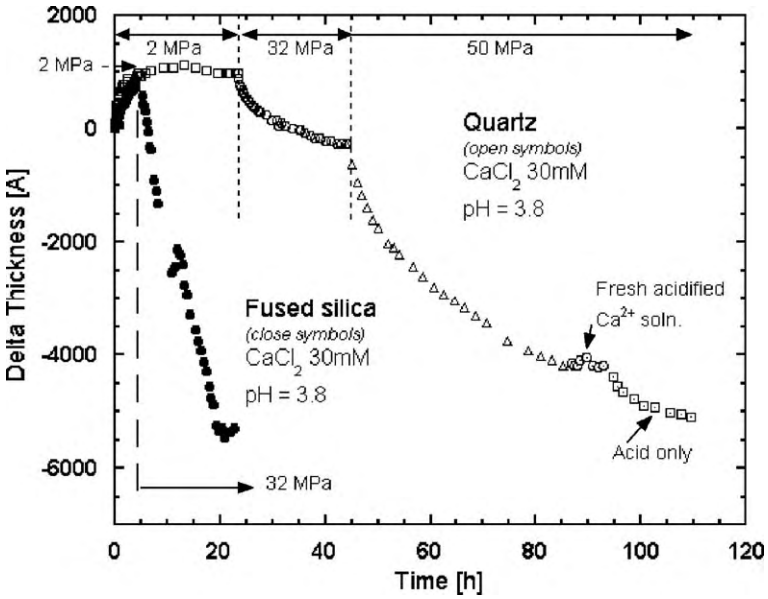

Fig. 5. Change of thickness vs. time for asymmetric surfaces experiments. The plot on the left corresponds to fused silica–mica surfaces. The data to the right corresponds to the quartz–mica surfaces. The surfaces were exposed to different electrolyte conditions as shown on the top. The regions for the three different pressures are noted by the small-dash lines.

at this higher pressure experienced an additional decrease of thickness of ca. 3800 Å. The dissolution is twofold, an initially fast process and a slow process that reaches a plateau at the 86 h mark. At this point, 150 ml of fresh acidic calcium chloride solution from the same batch as before was cycled through the SFA. The injection of fresh solution produced a fluctuation in the thickness of the fluid between the surfaces. The pressure from the previous experiment was kept constant for the remainder of the experiments.

The SFA was drained, purged several times with a diluted nitric acid solution of pH 3.8, and subsequently filled with this acidic solution for the last part of the experiment. The thickness changed approximately 700 Å in a lapse of 15 h. This thickness reduction seems slower than the observed values for the acidified calcium chloride solution, suggesting that the $CaCl_2$ electrolyte solution plays an important role in the kinetics of the dissolution.

The surfaces of mica and quartz crystal were studied with E-SEM once the experiments were concluded. The mica surfaces always looked featureless. Fig. 6 shows most of the contact surface area on the silica crystal. The final area of contact on the quartz sheet is greater than 250–350 μm. We believe that the surface of contact moved steadily from the original position every time a new pressure was applied. This may be caused by a horizontal creep produced by a slight deflection of the cantilever springs of the SFA that shifted the contact area from its original position at $t=0$ min.

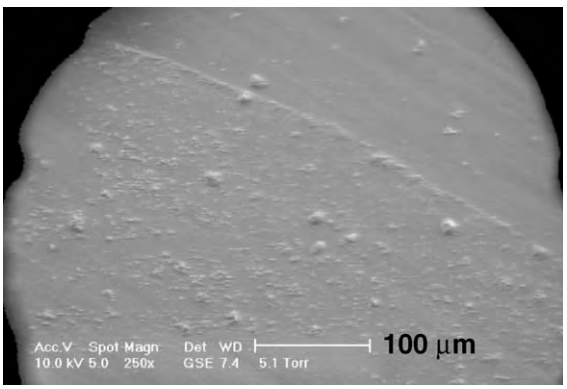

Fig. 6. E-SEM image of the contact region on a Z-cut quartz surface that had been in contact with a mica surface for more than 110 h in the SFA. This image shows the reduced thickness and changed surface texture (pitting) of a Z-cut crystal sheet within the contact junction compared to the thicker, smoother region that was outside the contact area. The size of the contact area agrees with that visualized in situ with the optical (multiple beam Interferometry) technique in the SFA experiments. This image is direct evidence of quartz dissolution owing to close contact with mica.

4. Discussion and conclusions

A number of novel conclusions can be drawn from our studies that may also apply to other mineral surfaces.

(i) Electrolyte type definitely has a great effect on the adhesion forces at the contact between mineral surfaces. This and the additional effects of pH on the surface charge and hydration and solvent-structural forces are important to determine the dissolution and diffusion process at the contact between similar or dissimilar surfaces. The equilibrium water gap thicknesses for lithostatic pressures up to 500 atm range from 0 (or about one layer of water molecules) to ~30 Å in mica–mica. In the case of mica–quartz system, the separation thickness increases in the first 4 h when the lithostatic pressure is very small. This slight confinement allows almost free diffusion and exchange of ions and water into and out of these gaps.

(ii) The diffusion of water or ions into or out of the film is not prevented whether the water is "structured" or not. Hydrated ions such as Na^+ were found to rapidly enter into a film that is initially thinner than the hydrated diameter of the ion, and the even more hydrated calcium ion can still enter into a highly structured water film (Fig. 3) with a diffusion coefficient that is not very different from its value in bulk water. Thus, the idea that structured water at or between two surfaces can lower the diffusivity by many orders of magnitude is not supported by our direct measurements, at least between two mica surfaces. This work concluded that diffusion through ultra-thin water films may not always be the rate-limiting step in pressure solution and instead the rates of ion exchange and local dissolution or crystal growth at dissolution or nucleation sites may be the rate limiting step(s).

(iii) We also found that the rate-limiting step for binding or crystal growth is not the rate at which ions reach their binding site but the binding itself, which presumably involves an exchange of two hydrated species. In order to bind, the guest ion must first divest itself of its hydration shell (or part of it) while the host ion must remove itself from the surface to which it is bound. Since both ions are initially tightly bound, the first to water and the other to the surface binding site, the activation barrier for the exchange can acceptably be assumed to be high and rate-limiting.

(iv) Our results show that by recording the changing shape, thickness, and contact area with time following a change in the surrounding solution it is possible to monitor and distinguish between diffusion and binding. The results shown in Fig. 3 clearly indicate that diffusion occurs more rapidly than binding (or surface exchange) of ions, at least in the case of calcium exchanging with sodium or protons on the surface. This ability to distinguish between different processes going on simultaneously but at different rates should allow for much greater insights on the fine details of the different stages during pressure solution.

(v) In the case of dissimilar surfaces there is an initial stage after fresh solution or acidic calcium solution is added in which an increase in the interferometer thickness is observed. Addition of fresh solution later in the experiment shows a similar effect on the process.
- For a particular set of conditions, the process slows down and reaches equilibrium after some time. An increase of pressure at this point increases the rate of pressure solution.
- This study shows that pressure has an important effect on pressure solution. At higher pressures, the thickness decreases to a larger extent than at low pressure, taking longer time for the process to achieve equilibrium.
- Pressure solution for this system is highly dependent upon interfacial solution composition. From the results presented in this paper we can infer that calcium and pH play an important role for the case under study; the presence of calcium and/or low pH accelerate pressure dissolution of silica for the mica–quartz system.
- Physical evidence of the dissolution of the silica can be observed using E-SEM. This evidence shows itself as an area of modified roughness with an elliptical shape.

(vi) The dissolution of fused silica is quite different than quartz which is not surprising given that amorphous silica has a higher solubility than crystalline quartz (Rimstidt and Barnes, 1980). Our results indicate that the dissolution rates are much higher as well, and this may be due at least in part to the close proximity of the muscovite mica surface. While almost the same amount of silica thickness was lost over a period of 24 h at 32 MPa, removal of material in the case of the amorphous silica took only 15% of the time that was needed for the Z-cut quartz to dissolve at the same pressure. This is a direct indication of the effect of the crystal array. Additionally, the same noticeable increase of thickness in the early stages of the experiment occurred for both types of silica (quartz and amorphous). This could be due to an initial hydration or separation that last for about 4 h due to the injection of the electrolyte solution. We were not able to monitor higher pressure effects because the acid affected the silver layer and the FECO patterns were no longer visible.

(vii) The rates of dissolution after several hours slow down after several hours, indicating a possible saturation of the bulk solution by quartz or fused silica. However, the solubility of quartz has been determined to be between 110 and 180 μmol/L at 25 °C (Rimstidt and Barnes, 1980; Fournier and Potter, 1982). This range of values is far from the saturation value of the bulk solution that can be attained in the SFA chamber (volume ~ 150 mL). However, it may be that there is a local dissolution process that in fact may happen just on the surface of the contact. Therefore, the contact position and its shape may be also a factor in the dissolution process. The effect of other factors such as temperature, shape of contact, and electrolyte solution is currently under investigation.

4.1. Implications of results for understanding pressure solution mechanisms

Our results on mica symmetrical surfaces alone do not allow us to determine precisely the mechanism of pressure solution. However, in the experiments with *asymmetric* systems such as quartz against mica we observed slow surface dissolution of quartz under different solution conditions and applied pressures. These phenomena did not occur at mica–mica contacts.

Our results show that diffusion is not the rate-limiting step to pressure solution. Rather, the rate of ion exchange and the lithostatic pressure would have more effect in local dissolution or crystal growth at the dissolution or nucleation site. We are continuing these experiments with quartz–quartz and with other phyllosilicate surfaces such as biotite.

Acknowledgements

We thank Dr. Jose Saleta for his help with the ESEM imaging. Dr. Saleta is in charge of the Micro-Environmental Imaging and Analysis Facility of the Donald Bren School of Environmental Science and Management, UCSB. This work was supported by NSF grant EAR 0342796 and the American Chemical

Society's Petroleum Research Fund (PRF grant No. 39823-AC2). **[DR]**

References

Alcantar, N., Israelachvili, J., Boles, J., 2003. Forces and ionic transport between mica surfaces: implications for pressure solution. Geochimica Et Cosmochimica Acta 67 (7), 1289–1304.

Bjørkum, P.A., 1996. How important is pressure in causing dissolution of quartz in sandstones? Journal of Sedimentary Research 66 (1), 147–154.

Christenson, H.K., Horn, R.G., et al., 1982. Measurement of forces due to structure in hydrocarbon liquids. Journal of Colloid and Interface Science 88 (1), 79–88.

Christenson, H.K., Israelachvili, J.N., Pashley, R.M., 1987. Properties of capillary fluids at the microscopic level. SPE Reservoir Engineering 2 (2), 155–165.

den Brok, S., 1998. Effect of microcracking on pressure-solution strain rate: the Gratz grain-boundary model. Geology 26 (10), 915–918.

Fournier, R.O., Potter, R.W., 1982. An equation correlating the solubility of quartz in water from 25-degrees-C to 900-degrees-C at pressures up to 10,000 bars. Geochimica Et Cosmochimica Acta 46 (10), 1969–1973.

Frens, G., Overbeck, J.T., 1972. Repeptization and theory of electrostatic colloids. Journal of Colloid and Interface Science 38 (2), 376–387.

Gardella, J., 1995. Secondary ion mass spectroscopy. The handbook of surface imaging and visualization. A. Hubbart. Boca Raton, CRC Press.

Guldbrand, L., Jonsson, B., et al., 1984. Electrical double layer forces. A Monte Carlo study. Journal of Chemical Physics 80 (5), 2221–2228.

Heald, M.T., 1955. Stylolites in sandstones. Journal of Geology 63, 101–114.

Heuberger, M, Luengo, G., Israelachvili, J., 1997. Topographic information from multiple beam interferometry in the surface forces apparatus. Langmuir 13 (14), 3839–3848.

Hochella Jr., M.F., 1995. Mineral surfaces: their characterization and their chemical, physical and reactive nature. Mineral. Soc. Ser. R. A. D. Vaughan and Pattrick, 5. Chapman and Hall Publishers, London, pp. 17–60.

Israelachvili, J., 1973. Thin-film studies using multiple-beam interferometry. Journal of Colloid and Interface Science 44 (2), 259–272.

Israelachvili, J., 1991. Intermolecular and Surface Forces. Academic Press Limited, San Diego, CA.

Israelachvili, J., Adams, G.E., 1978. Measurement of forces between 2 mica surfaces in aqueous-electrolyte solutions in range 0–100 nm. Journal of the Chemical Society. Faraday Transactions I 74, 975–1001.

Kekicheff, P., Marcelja, S., et al., 1993. Charge reversal seen in electrical double layer interaction of surfaces immersed in 2:1 calcium electrolyte. Journal of Chemical Physics 99 (8), 6098–6113.

Kjellander, R., Marcelja, S., et al., 1988. Double-layer ion correlation forces restrict calcium-clay swelling. Journal of Physical Chemistry 92 (23), 6489–6492.

Kjellander, R., Marcelja, S., et al., 1990. A theoretical and experimental study of forces between charged mica surfaces in aqueous calcium chloride solutions. Journal of Chemical Physics 92 (7), 4399–4407.

Kruzhanov, V., Stöckhert, B., 1998. On the kinetics of elementary processes of pressure solution. Pure and Applied Geophysics 152 (4), 667–683.

Leckband, D., Israelachvili, J., 2001. Intermolecular forces in biology. Quarterly Reviews of Biophysics 34 (2), 105–267.

Li, Y.H., Gregory, S., 1974. Diffusion of ions in sea-water and in deep-sea sediments. Geochimica Et Cosmochimica Acta 38 (5), 703–714.

Pashley, R.M., 1981. DLVO and hydration forces between mica surfaces in lithium, sodium, potassium, and cesium ions electrolyte solutions: a correlation of double-layer and hydration forces with surface cation exchange properties. Journal of Colloid and Interface Science 83 (2), 531–546.

Pashley, R.M., 1982. Hydration forces between mica surfaces in electrolyte solutions. Advances in Colloid and Interface Science 16, 57–62.

Pashley, R.M., Israelachvili, J.N., 1984. DLVO and hydration forces between mica surfaces in magnesium(2+), calcium(2+), strontium (2+), and barium(2+) chloride solutions. Journal of Colloid and Interface Science 97 (2), 446–455.

Renard, F., Ortoleva, P., 1997. Water films at grain–grain contacts: Debye-Huckel, osmotic model of stress, salinity, and mineralogy dependence. Geochimica Et Cosmochimica Acta 61 (10), 1963–1970.

Renard, F., Park, A., et al., 1999. An integrated model for transitional pressure solution in sandstones. Tectonophysics 312, 97–115.

Rimstidt, J.D., Barnes, H.L., 1980. The kinetics of silica–water reactions. Geochimica Et Cosmochimica Acta 44 (11), 1683–1699.

Rutter, E.H., 1983. Pressure solution in nature, theory and experiment. Journal of the Geological Society of London 140, 725–740.

Sherwood, P., 1995. X-ray photoelectron spectroscopy. The handbook of surface imaging and visualization. A. Hubbart. Boca Raton, CRC Press.

Tada, R., Maliva, R., et al., 1987. A new mechanism of pressure solution in porous quartzone sandstone. Geochimica Et Cosmochimica Acta 51, 2295–2301.

van Olphen, H., 1977. An Introduction to Clay Colloid Chemistry. Wiley, New York.

Verwey, E., Overbeek, J.T.G., 1948. The theory of the stability of lyophobic colloids. Amsterdam, Elsevier.

Viani, B.E., Low, P.F., et al., 1983. Direct measurement of the relation between interlayer force and interlayer distance in the swelling of Montmorillonite. Journal of Colloid and Interface Science 96 (1), 229–244.

Vigil, G., Xu, Z., Steinberg, S., Israelachvili, J., 1994. Interactions of silica surfaces. Journal of Colloid and Interface Science 165 (2), 367–385.

Wan, K.T., Lawn, B.R., et al., 1992. Repulsive interaction between coplanar cracks in the double - cantilever geometry. Journal of Materials Research 7 (6), 1584–1588.

Weyl, P.K., 1959. Pressure solution and the force of crystallization—a phenomenological theory. Journal of Geophysical Research 64, 2001–2025.